

## TRANSCRIPTOME SEQUENCING AND ANALYSIS OF ATRAZINE STRESS ON *SUAEDA SALSA*

LU, H. B. – WEI, H. F.\*

*Dalian Ocean University, Dalian, China*  
(*e-mail: 15293557967@163.com – H. B. Lu*)

*\*Corresponding author*  
*e-mail: weihaifeng@dlou.edu.cn*

(Received 1<sup>st</sup> Apr 2022; accepted 26<sup>th</sup> Jul 2022)

**Abstract.** Pesticides are an indispensable part of agricultural production, and herbicides are more widely used in agriculture. Through the hydroponic experiment, it was found that atrazine would affect the growth of *Suaeda salsa*. High throughput sequencing was used to analyze its transcriptome in order to explain the growth pathway of atrazine on *Suaeda salsa* at molecular level. A total of 78.92 g data were obtained by transcriptome sequencing of *Suaeda salsa*, 443515 transcripts with an average length of 998 BP were obtained, and 261694 unigenes with an average length of 864 BP were obtained by splicing. All unigenes were annotated with seven databases, and 195917 unigenes were annotated successfully in at least one of the above seven databases, accounting for 74.86% of the total unigenes. The results of differential analysis were analyzed by KEGG pathway enrichment analysis. The results showed that the processes of significant enrichment of high, medium and low atrazine concentrations compared with the control group were ribosome, phagosome and oxidative phosphorylation. The transcription and translation related genes of elongation factor in ribosomes and SecY membrane protein related genes producing protein membrane channels were up-regulated, the F-actin and V-ATPase related genes involved in transport in phagocytes were up-regulated, and the f-atpase and V-ATPase related genes producing ATP during oxidative phosphorylation were up-regulated, indicating that the above related genes were involved in the corresponding response to atrazine stress.

**Keywords:** *Suaeda salsa*, transcriptional response, atrazine stress, molecular level

### Introduction

Atrazine is a triazine herbicide with low production cost and good herbicidal effect (Ge et al., 2021; Yan et al., 2015). However, the structural stability and non-degradable nature of atrazine can cause it to stay in the soil for a long time. Therefore, atrazine can be toxic to sensitive crops (Mali et al., 2021). In addition, atrazine has water-soluble properties. Therefore, atrazine present in the soil that cannot be decomposed in a short time is easily dissolved in rainwater and agricultural irrigation water, or seeps into the ground or sinks into rivers. Eventually, it causes pollution and damage to the ecosystem (Bachetti et al., 2021). In summary, it is reasonable to speculate that atrazine affects chemical and biological processes in the soil environmental system. It was found (Zhang et al., 2017; Rohr, 2021) that atrazine affects the normal growth and development of crops, the structural composition of soil microbial communities and the transformation of substances in the soil, ultimately causing pollution of the environment.

Atrazine mainly enters the plant body through the roots and leaves of root plants and the cell surface of unicellular plants. Atrazine blocks the binding of D1 protein to plastoquinone by acting as an inhibitor of plastoquinone binding, thereby blocking electron transfer in photosynthetic system II. This blockage would lead to chlorophyll destruction and termination of carbohydrate synthesis, thus inhibiting photosynthesis

(Karim et al., 2021). At the same time, the oxidative stress and free radical production caused by the blockage of electron transfer can cause massive and rapid cellular damage, which can lead to plant decay and death (Kumari et al., 2021; James and Kumar, 2021). Current studies have shown that higher concentrations of atrazine have a strong toxic effect on aquatic vascular plants (Li et al., 2008). In addition, when the concentration of atrazine was above 0.1 mg/L, it significantly affected the photosynthesis and chlorophyll content of aquatic plants (Alberto et al., 2016). The effects of atrazine on chlorophyll content, antioxidant enzyme activity and chlorophyll content of reed were investigated by hydroponic experiments. The results showed that southern reed was tolerant when the atrazine concentration was less than or equal to 8 mgL<sup>-1</sup>, but the growth of southern reed was stopped after 2 weeks of stress (Qi et al., 2014). Liu et al. (2011) investigated the response of the symbiotic system of the bush mycorrhizal fungus Cannon to atrazine stress. The results showed that atrazine stress inhibited the growth and development of plantain. Atrazine stress reduced photosynthetic rate, transpiration and stomatal conductance of plantain roots. Thus, this stress caused damage to the cellular and subcellular structure and also led to the occurrence of intracellular antioxidant stress responses, which in turn affected the growth and photosynthesis of plantain.

*Suaeda salsa* is an annual herb belonging to the genus *Suaeda* in the family Lycidae. It grows in coastal, lakeside, desert and other saline alkali land. It is a pioneer plant developing from land to coast and is also a typical saline alkali indicator plant (Su et al., 2018). *Suaeda salsa* is 20-90 cm in height, with red stems and leaves which are slightly fleshy, elongated (Kang et al., 2021). However, with the influence of human activities in recent years, *Suaeda salsa* has died in a large area in Panjin red beach, Liaoning Province, in China. After extensive preliminary research, it was found that atrazine does exist in the seawater and in the soil of Panjin Red Beach (Liu et al., 2020). In conclusion, atrazine has a toxic effect on *Suaeda salsa*, but the effect of atrazine on the gene expression of *Suaeda salsa* is still unclear. Therefore, this study analyzed the transcriptomic response of *Suaeda salsa* to atrazine stress. The differences in gene expression of *Suaeda salsa* at different atrazine concentrations were analyzed. The aim of this paper is to find a theoretical basis for the mass mortality of Panjin Red Beach and to provide a reference for the ecological restoration of Panjin Red Beach.

## Materials and methods

### *Plant material and culture*

*Suaeda salsa* seeds were purchased from Panjin City, Liaoning Province. The herbicide atrazine was produced by Jiangsu Ruibang Pesticide Factory Co., Ltd. (the content of effective components was 90%, and the dosage form was water dispersible granule).

The experiment was carried out in Liaoning Key Laboratory of coastal marine environmental science and technology, Dalian Ocean University. In the experiment, *Suaeda salsa* seedlings with the same growth time and similar plant height were cleaned in the form of hydroponics. The roots were washed with deionized water. The cleaned *Suaeda salsa* seedlings were put into a beaker containing Hogland nutrient solution. The beaker was placed in a light incubator. The light cycle was 12 h, the temperature was controlled at 20 °C, and the light intensity was 6480 lux, stable for 3 days. The consumed nutrient solution was supplemented every day.

Three days later, atrazine solution was prepared with Hogland nutrient solution. By reviewing the relevant literature and the results of field monitoring of atrazine, three concentrations were determined: high, medium and low, respectively, for the control group (C, 0 mg/L), low concentration group (L, 0.1 mg/L), medium concentration group (M, 0.4 mg/L) and high concentration group (H, 1 mg/L). Stable *Suaeda salsa* seedlings were put into atrazine solutions with different concentrations. About 20 seedlings were placed in each concentration. Three seedlings were placed in each experimental group in parallel. The nutrient solution was changed every 4 days to keep atrazine concentration unchanged. The experimental period was 6 days. The control group and three concentration gradient samples are represented by C, l, m and h, respectively. Due to the existence of parallel experiments, the results are represented as C-1, C-2, C-3, L-1, L-2, L-3, M-1, M-2, M-3, H-1, H-2 and H-3, with a total of 12 samples. The samples were frozen in liquid nitrogen for sequencing analysis. Immediately after collection, the samples were placed in precooled RNAiso, then refrigerated in dry ice and sent to Novo Zhiyuan for RNA extraction and sequencing.

### ***Sample collection and RNA extraction***

RNA was extracted using a Trizol kit (Invitrogen, CS, USA) according to standard procedures. RNA degradation and contamination was monitored on 1% agarose gels. The purity and integrity of RNA were detected by Nanodrop and Agilent 2100 respectively. RNA concentration was measured using Qubit® RNA Assay Kit in Qubit® 2.0 Fluorometer (Life Technologies, CA, USA).

### ***Library preparation and sequencing***

The transcriptome library was prepared according to the procedure described in the previous report (Kang et al., 2020). The library building starting RNA was total RNA, and mRNA with polyA tails was first enriched by Oligo (dT) magnetic beads, followed by random interruption of the obtained mRNA with divalent cations in Fragmentation Buffer. Using the fragmented mRNA as a template and random oligonucleotides as primers, the first strand of cDNA was synthesized in the M-MuLV reverse transcriptase system, followed by degradation of the RNA strand with RNaseH and synthesis of the second strand of cDNA with dNTPs under the DNA polymerase I system. The purified double-stranded cDNA was end-repaired, A-tailed and connected to the sequencing junction, and the cDNA of about 370~420 bp was screened with AMPure XP beads, PCR amplified, and the PCR products were purified again with AMPure XP beads to finally obtain the library. After the library was constructed, the library was initially quantified using a Qubit 2.0 Fluorometer and diluted to 1.5 ng/ul, and then the insert size of the library was detected using an Agilent 2100 bioanalyzer, and after the insert size was as expected, the effective concentration of the library was accurately quantified by qRT-PCR. After the insert size met the expectation, qRT-PCR was performed to accurately quantify the effective concentration of the library (effective library concentration above 2 nM) to ensure its quality.

After passing the library test, different libraries are pooled according to the effective concentration and the target downstream data volume and then sequenced by Illumina, and 150 bp paired-end reads are generated. The basic principle of sequencing is Sequencing by Synthesis.

### ***Transcriptome assembly and gene functional annotation***

The raw image data files obtained by high-throughput sequencing were converted into sequenced reads (raw reads) by the CASAVA Base Calling analysis. After the raw reads were obtained, the sequencing error rate was first evaluated by Qphred (Q20 and Q30 respectively indicate that the base correct recognition rate is 99%, 99.9%); in addition, the presence or absence of the AT and GC separation phenomenon was detected by the GC content distribution. Clean reads were obtained from raw reads by removing reads containing adapter,  $N > 10\%$  ( $N$  indicates the base could not be determined) and low-quality reads. After obtaining clean reads, the clean reads were spliced by Trinity. The transcript sequence obtained by splicing was used as reference sequence for subsequent analysis.

Gene function annotations for transcript were performed based on seven databases, including: Nr, Nt, Pfam, KOG/COG, Swiss-prot, KEGG, GO. Among them, NR, KOG/COG and Swiss-Prot were annotated with software diamond; NT, KEGG, Pfam, GO were annotated by software NCBI blast, KAAS, hmmscan and Blast 2 GO respectively.

### ***Differential expression analysis***

Gene expression analysis was performed by RSEM. Using software Bowtie2 with parameter mismatch 0 (default). Prior to differential gene expression analysis, for each sequenced library, the read counts data obtained from gene expression analysis were adjusted by edgeR program package through one scaling normalized factor as described in the previous report (Mevy et al., 2020). Differential expression analysis of two samples was performed using the DEGseq (2010) R package, and  $P < 0.005$  &  $|\log_2(\text{Fold Change})| > 1$  was set as the threshold for significantly differential expression. GO enrichment of differentially expressed genes was performed on Goseq with the parameter  $P < 0.05$  (Chakrapani et al., 2016). KEGG enrichment was performed on differentially expressed genes using KOBAS with the parameter  $P < 0.05$  (Li et al., 2019).

## **Results**

### ***RNA-seq, data preprocessing and sequence assembly***

The raw data of control group C and experimental group L, M and H were sequenced. Raw reads of 12 samples ranged from 20.969 million to 23.919 million. The number of high-quality clean reads obtained by filtration ranged from 20.642 million to 23.436 million. The total number of clean bases in 12 groups reached 78.92 G. The error rate was 0.02% except for C-3 and M-3, which were 0.03%; The contents of Q20, Q30 and GC are shown in *Table 1*.

After processing by Trinity software, a total of 443,515 transcripts were obtained, with an average length of 998 bp and a maximum length of 15,773 bp for N50 and N90. Among them, the number of transcripts between 300-500 bp was 175,499. Finally, after double-end information assembly, the longest transcript of each gene was selected as a single gene, and a total of 261,694 single genes were obtained, with an average length of 864 bp and a maximum length of 15,773 bp. the number of single genes between 300 and 500 bp was 110,356, and N50 and N90 were 1,117 bp and 404 bp, respectively. The frequency distribution of splice length and splice distribution of the lengths are shown in *Tables 2* and *3*.

**Table 1. Sequencing data quality**

Sample	Raw reads	Clean reads	Clean bases	Error (%)	Q20 (%)	Q30 (%)	GC (%)
C_1	21921679	21385313	6.42G	0.02	98.24	94.58	42.53
C_2	21865080	21336345	6.4G	0.02	98.32	94.82	42.31
C_3	22549184	22000121	6.6G	0.03	97.8	93.54	42.3
L_1	22050991	21370452	6.41G	0.02	98.2	94.53	43.32
L_2	22967081	22421164	6.73G	0.02	98.25	94.67	43.99
L_3	23513368	23076060	6.92G	0.02	98.34	94.84	42.74
M_1	23919239	23435778	7.03G	0.02	98.21	94.53	42.43
M_2	22607574	22048616	6.61G	0.02	98.15	94.39	42.73
M_3	21423335	21101407	6.33G	0.03	98.04	94.12	42.12
H_1	23473927	23056249	6.92G	0.02	98.35	94.92	47.51
H_2	21570548	21200975	6.36G	0.02	98.25	94.67	45.53
H_3	20969253	20642107	6.19G	0.02	98.19	94.45	42.64

Clean bases: the number of sequenced sequences multiplied by the length of sequenced sequences, and converted to the unit of G; Error (%): sequencing base error rate; Q20, 30 (%): the percentage of bases with phred values greater than 20 and 30 in total bases; GC content (%): the percentage of the total number of bases g and C in the total number of bases

**Table 2. Splicing length frequency distribution**

Transcript length interval	300-500 bp	500-1 kbp	1 k-2 k bp	>2 k bp	Total
Number of transcripts	175499	128559	85922	53535	443515
Number of unigenes	110356	88052	42487	20799	261694

**Table 3. Splicing length distribution**

	Min length	Mean length	Median length	Max length	N50	N90	Total nucleotides
Transcripts	301	998	615	15773	1485	418	442633466
Unigenes	301	864	562	15773	1117	404	226195038

N50, N90: the spliced transcripts are sorted according to the length from large to small, and the length of the spliced transcripts is accumulated to the length of no less than 50%/90% of the total length, which is N50/N90

### Gene function annotation

Since there is no genome-wide background of *Suaeda salsa*, we compared 261694 single genes with known public databases NR, NT, Swiss, Protein, Pfam, KEGG, COG and counted the number of single genes annotated in each database by BLASTN and BLASTX to complete the annotation of *Suaeda salsa* genes and prediction of function. By comparing with the above seven databases, 147,649, 89,782, 74,786, 129,562, 137,391, 137,383 and 80,756 unigenes were able to obtain homology comparison information, accounting for 56.42%, 34.3%, 28.57%, 49.5%, 52.5%, 52.49% and 30.85%, respectively. And at least one of the above seven databases successfully annotated 195917 single genes, accounting for 74.86% of the total number of single genes (Table 4).

**Table 4.** Gene annotation success rate statistics

	Number of Unigenes	Percentage (%)
Annotated in NR	147649	56.42
Annotated in NT	89782	34.3
Annotated in KO	74786	28.57
Annotated in SwissProt	129562	49.5
Annotated in PFAM	137391	52.5
Annotated in GO	137383	52.49
Annotated in KOG	80756	30.85
Annotated in all Databases	27840	10.63
Annotated in at least one Database	195917	74.86
Total Unigenes	261694	100

### Gene differential expression analysis

Compared with the control group, a total of 33,907 differential genes were generated in experimental group H, of which 33,370 were up-regulated and 537 were down-regulated; a total of 8,450 differential genes were generated in experimental group M, of which 7,303 were up-regulated and 1,147 were down-regulated; a total of 15,832 differential genes were generated in experimental group L, of which 14,791 were up-regulated and 1041 genes were down-regulated (Fig. 1).

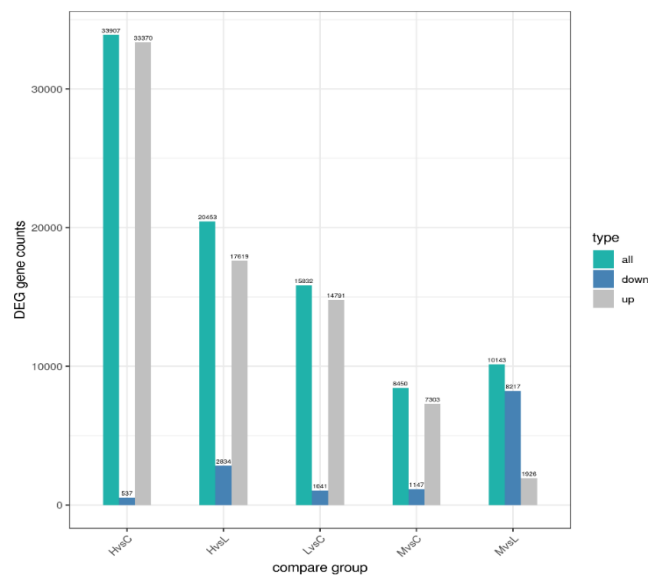


**Figure 1.** Number of differential genes

Differentially expressed transcripts in the three experimental groups were found to increase with increasing concentrations of atrazine (Fig. 2). There were 10216 differentially expressed transcripts in the group L, 2183 differentially expressed transcripts in the group M and 26691 differentially expressed transcripts in the group H. This indicates that the *Suaeda salsa* transcriptional responds more to the stress of high concentration of atrazine.

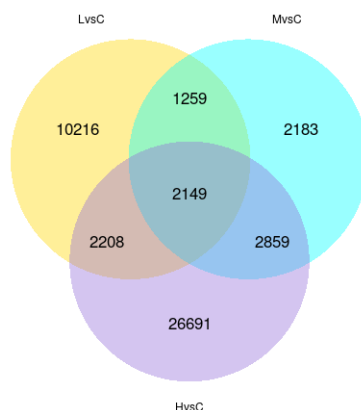


**Figure 2.** Venn of differentially expressed transcripts. The sum of the numbers in each circle represents the number of differentially expressed transcripts in a group, the intersecting part represents the differentially expressed transcripts contained in each group, and the non intersecting part is the unique differentially expressed transcripts of the group

### ***GO enrichment analysis of differentially expressed genes***

Differential transcriptome expression under high concentration of atrazine stress (group H, Fig. 3a). The most up-regulated differential genes occurred in cellular and cellular fractions, both with 7077, followed by intracellular fraction and intracellular with 6644 and 6678, respectively; under the classification of biological processes, the most up-regulated differential genes occurred in biosynthetic processes and organic matter biosynthesis, with 6264 and 6040, respectively; under the classification of molecular functions, the largest number of differential genes were found in oxidoreductase activity, structural activity and structural components of ribosomes, with 2193, 2035 and 1676 differential genes, respectively.

### ***Differential transcriptome expression under medium concentration of atrazine stress (group M, Fig. 3b)***

Under the cellular component the most differential genes with upregulation occurred in the cell and cellular fraction, both with 1944, followed by the intracellular fraction and intracellular with 1839 and 1847, respectively; under the biological process classification, the most differential genes with upregulation occurred in the biosynthetic process and organic matter biosynthesis with 1699 and 1651, respectively; under the molecular function classification, structural molecular activity and under the classification of molecular functions, the largest number of differential genes were found in the structural molecular activity and structural components of ribosomes, with 776 and 678 differential genes, respectively.

### ***Differential transcriptome expression under stress of low concentration of atrazine (group L, Fig. 3c)***

Under the cellular composition classification, the most differential genes were up-regulated in cells and cellular fractions, both with 3960; in the biological processes metabolic processes were up-regulated with 6698, followed by nitrogen compound metabolic processes and cellular nitrogen compound metabolic processes with 4135 and 2469, respectively; under the molecular function classification, the most differential genes were up-regulated in catalytic activity with 5438.

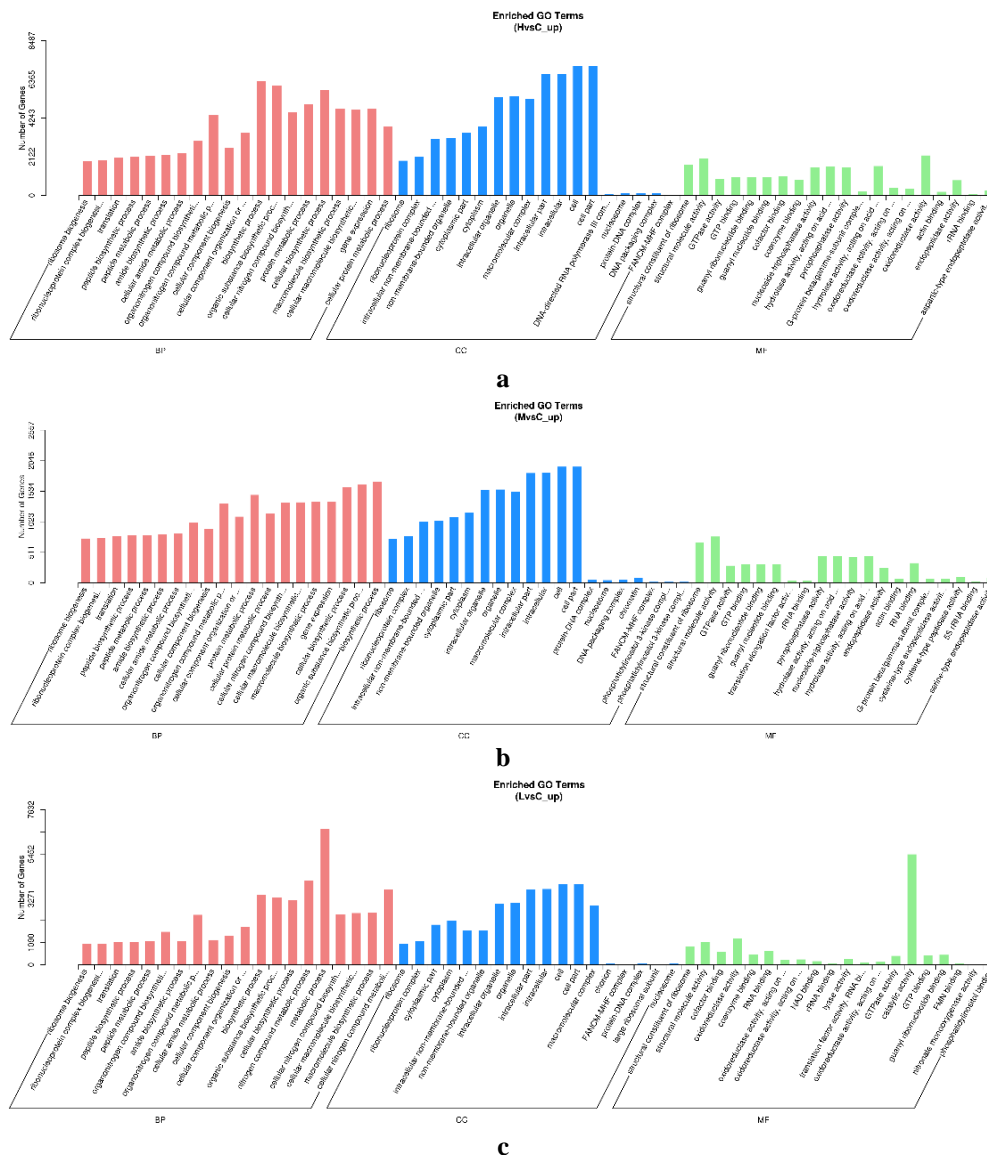


**Figure 3.** The GO enrichment analysis result for (a) group H, (b) group M and (c) group L

### **KEGG enrichment analysis of differentially expressed genes**

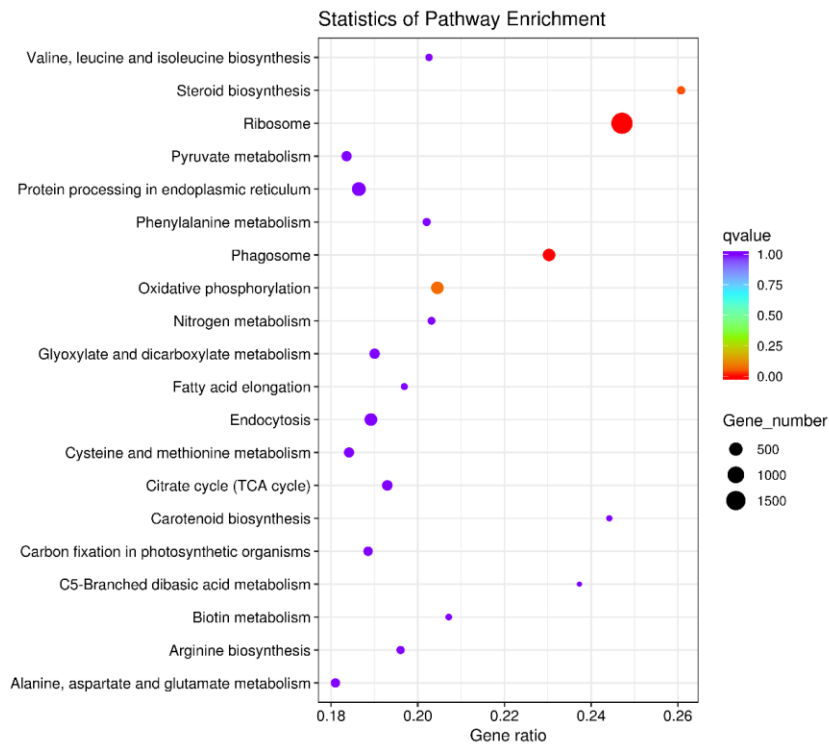
The results of the difference analysis were subjected to KEGG PATHWAY enrichment analysis, and it was found that the processes that were significantly enriched at high, medium and low atrazine concentrations compared to the control were (Fig. 4a, b, c): oxidative phosphorylation, steroid biosynthesis, photosynthesis and protein processing in endoplasmic reticulum.

### **Ribosomal pathway**

Among the main KEGG enrichment pathways, ribosome was significantly enriched in the three atrazine concentrations. As shown in Figure 5, through KEGG annotation, 142 unigenes in the transcriptome of *Suaeda salsa* were annotated into the KEGG pathway of ribosome under group H. Most of the genes were up-regulated including EF-Tu protein and SecY protein.

### Phagosome pathway

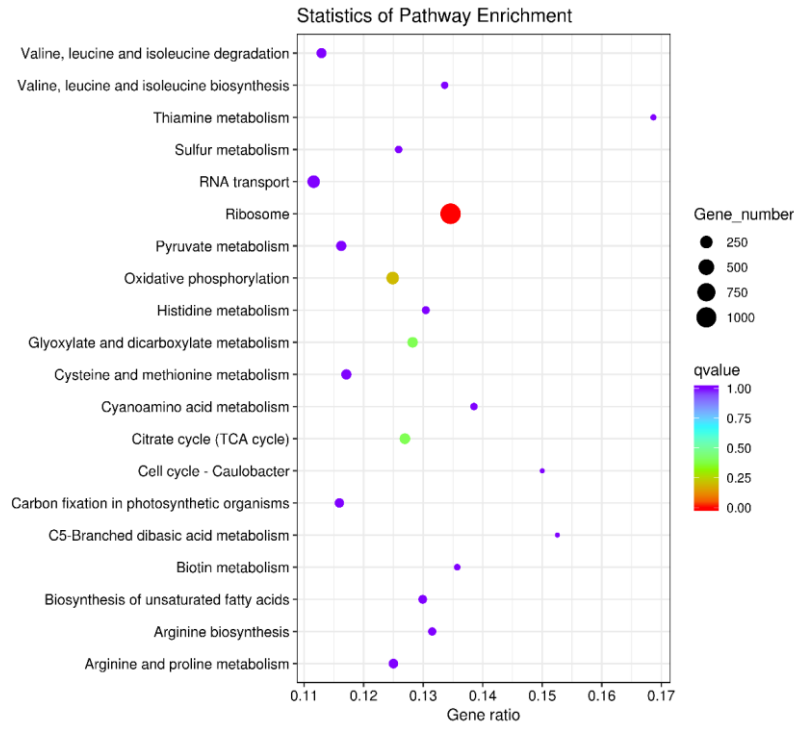
Through KEGG annotation, 73 unigenes were annotated into the KEGG pathway of phagosome under group H. As shown in *Figure 6*, 15 genes are up-regulated including V-ATPase, F-actin, F-actin, tuba protein.



**a**



**b**



c

Figure 4. The KEGG enrichment analysis result for (a) group H, (b) group M and (c) group L

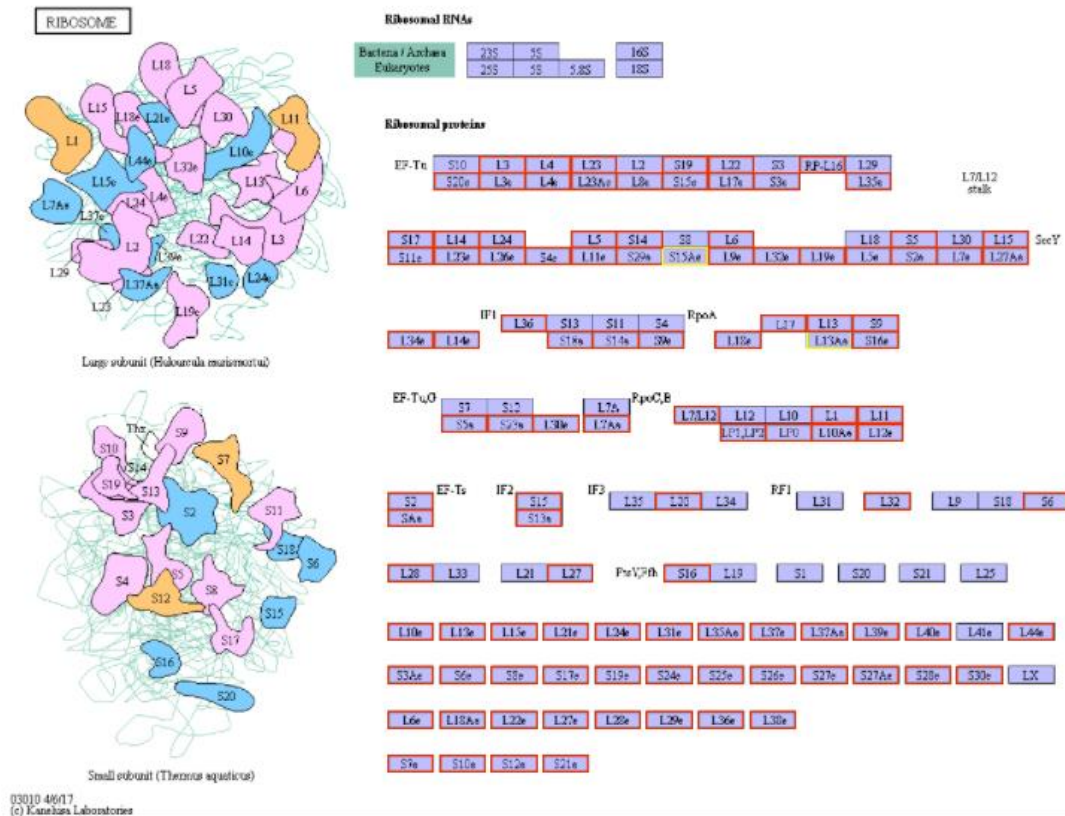


Figure 5. The ribosomal pathway of differential genes at group H

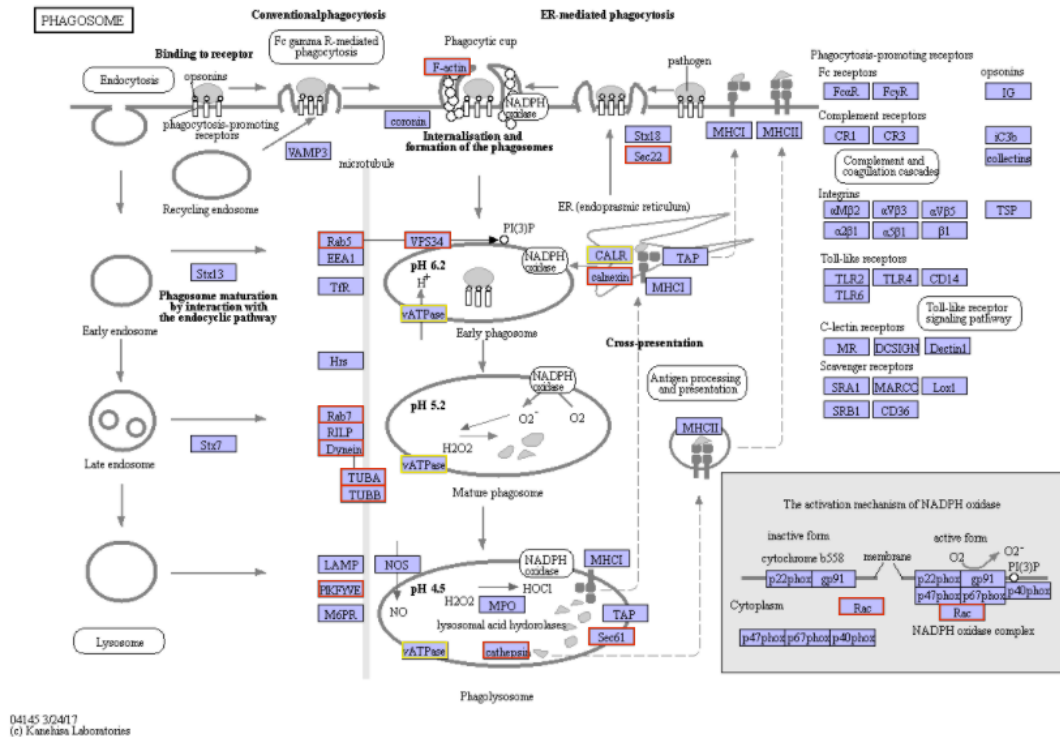


Figure 6. Differential gene phagosome pathway at group H

### Oxidative phosphorylation

Through KEGG annotation, we found that 192 unigenes were annotated into KEGG pathway of oxidative phosphorylation under group H. As shown in Figure 7, 62 genes are up-regulated, including NADH dehydrogenase, F-ATPase, V-ATPase.

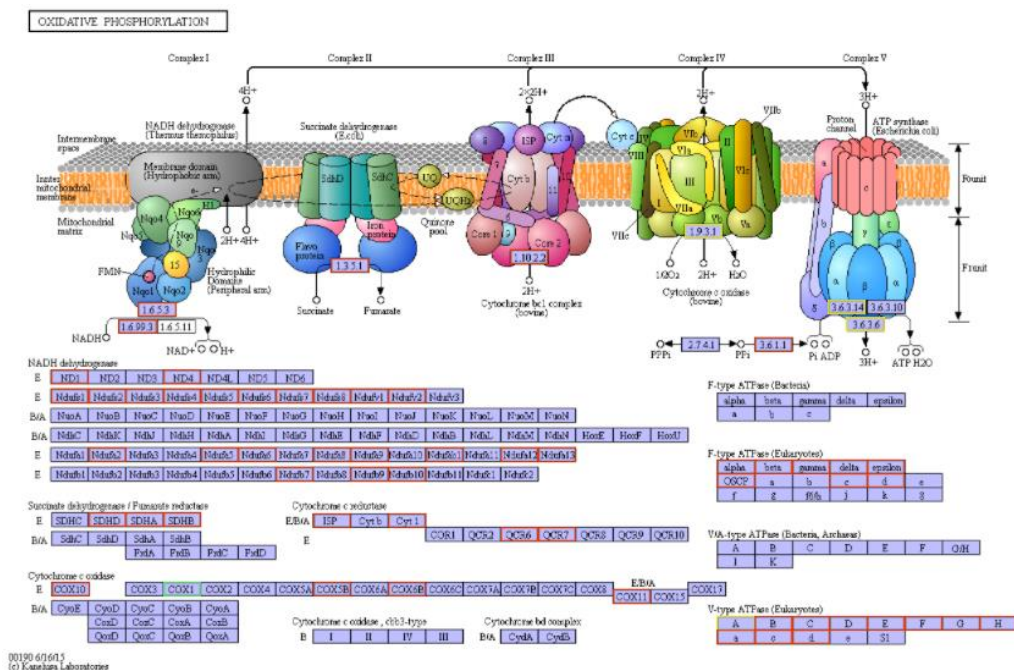


Figure 7. Pathways of oxidative phosphorylation of differential genes at group H

## Discussion

In this study, the effects of different concentrations of atrazine on the growth of *Suaeda salsa* under hydroponic conditions were studied, and the whole transcriptome of *Suaeda salsa* under the action of different concentrations of atrazine was sequenced by high-throughput sequencing technology. The results of differential analysis were enriched by KEGG path. The molecular regulation mechanism of atrazine in *Suaeda salsa* was studied from the level of metabolic pathway.

### *Ribosomal pathway regulation*

Elongation factor EF-Tu protein is an important protein involved in protein translation and extension (Cai et al., 2022). They promote and control protein synthesis by catalyzing the extension of amino acid chain on ribosome (Aviner, 2020; Wang et al., 2013). It is found that EF-Tu is the protein with the highest content among the proteins related to translation mechanism in cells (DeLey Cox et al., 2019). In addition, it also plays a very important role in growth signal transduction, heat resistance, drought resistance and disease resistance (Zhang et al., 2022; Fu et al., 2012). EF-Tu protein brings aminoacyl transfer RNA (tRNA) into ribosome in the extension stage of translation. EF-Tu • guanosine triphosphate (GTP) has high affinity with tRNA to form a ternary complex EF-Tu • GTP • tRNA. EF-Tu can recognize the common characteristics of tRNA and also recognize that tRNA is aminoacylated (Hughes, 2013). It is speculated that *Suaeda Heteroptera* has its own stress response under atrazine stress, resulting in the up regulation of EF-Tu protein related differential genes.

SecY is a membrane protein involved in the protein transport of cell membrane (Ma et al., 2019). The Sec system is the main pathway responsible for the export of proteins across the plasma membrane and the insertion of proteins into the plasma membrane. The Sec system is composed of membrane proteins SecY, sece and SecE, which form a channel on the cytoplasmic membrane for protein transport; Intracellular protein SecA mediates the transport of presecretory proteins into the channel through the energy of adenosine triphosphate (ATP) hydrolysis (Ma et al., 2019). Kakizawa et al. (2001) cloned SecA, SecY and sece genes from phytoplasma onion yellowing, and confirmed the existence of secretory protein transport system in phytoplasma. It is speculated that when atrazine stresses *Suaeda Heteroptera*, the stress response of self-protection produced by the body leads to the increase of EF-Tu protein in ribosome, which increases the SecY of transport protein and the up regulation of SecY related genes.

### *Phagosome pathway regulation*

A universal mechanism of V-ATPase is reversible decomposition (Hooper et al., 2022). Cells decompose in the absence of glucose, a mechanism for preserving cellular ATP during starvation. Recombination occurs rapidly after glucose recovery (McGuire and Forgac, 2018). However, experiments show that in some mammalian cells, V-ATPase assembly actually occurs under low sugar conditions and low amino acid availability conditions, which may be a mean to promote the circulation of biochemical building blocks through autophagy (Jaskolka and Kane, 2020; Eaton et al., 2021; Harvey, 1992). During the maturation of dendritic cells of the immune system, the assembly of V-ATPase on lysosomal membrane increases to stimulate antigen processing, which depends on the activity of protease, and it is the most effective at low pH (Stransky and Forgac, 2015). Studies have shown that in yeast, V-

atpases on vacuoles will increase under high extracellular pH or osmotic stress, which need to increase the transport of protons into vacuoles (Vasanthakumar and Rubinstein, 2020; Banerjee and Kane, 2020). F-Actin is an important cytoskeleton component in dendritic filamentous feet and processes, and it is involved in regulating the morphogenesis and synaptic plasticity of processes (Kim, 2009). In cells, the spiny end of F-actin faces the cell membrane, and the tip is fixed deep in the F-actin network. There, actin steps on a large scale, polymerizes directly below the membrane and depolymerizes at the rear of the F-actin network, thus providing power for membrane protrusions (Galkin et al., 2010; Ma and Tymanskyj, 2020). TUBA protein is a new scaffold protein. Its function is to bind dynein and actin regulatory protein together. It selectively binds dynein through four N-terminal SRC homology-3 (SH3) regions. TUBA protein binds to a variety of actins through the C-terminal SH3 domain. Forcibly targeting the C-terminal SH3 domain to the mitochondrial surface can promote the accumulation of F-actin around mitochondria (Wagh et al., 2015; Salazar et al., 2003).

### ***Oxidative phosphorylation***

Oxidative phosphorylation is the coupling reaction of ADP and inorganic phosphoric acid to synthesize ATP. NADH dehydrogenase is a protein composed of 42 subunits, of which 7 subunits are encoded by the mitochondrial genome (Ludwig et al., 2020; Burstein et al., 2000). NADH dehydrogenase is located in mitochondria and is called complex I during oxidative phosphorylation. Its main function is to transfer a pair of electrons to CoQ and 4 H<sup>+</sup> to the membrane gap. When protons return to the mitochondrial matrix, it drives ATP synthase to synthesize ATP (Braun, 2020; Manoj, 2018; Piccoli et al., 2008). NADH dehydrogenase subunit is located on the inner mitochondrial membrane, and its expression change can change the permeability of the inner mitochondrial membrane, thus changing the state of cytochrome c on the mitochondrial membrane, thus affecting the regulation of mitochondria on apoptosis (Manoj et al., 2020; Chen et al., 2009). Type F-ATPase is an ATPase/synthase that exists in bacterial plasma membrane, mitochondrial inner membrane (oxidative phosphorylation, which is called complex V there) and chloroplast thylakoid membrane. It uses a proton gradient to drive ATP synthesis, allows the passive flux of protons to pass through the membrane along its electrochemical gradient, and uses the energy released by the transport reaction to release the newly formed ATP from the active site of F-ATPase. Like V-ATPase and A-ATPase, F-ATPase belongs to the superfamily of related rotating ATPases (Chen et al., 2021; Kühlbrandt, 2019). F-ATPase mainly acts as ATP synthase and takes ADP and inorganic phosphate as substrates. It exists on the plasma membrane of eubacteria, the inner membrane of mitochondria and the thylakoid membrane of chloroplast. V-ATPase only acts as an ion pump driven by ATP hydrolysis and exists in various intracellular and interventricular membranes, such as chromatin granules, lysosomes, endosomes, synaptic vesicles, Golgi derived vesicles, yeast vesicles and plant vacuolar plastids. They are involved in many intracellular and intercellular processes, including receptor-mediated endocytosis, protein transport, pH maintenance and neurotransmitter release (Fan, 2009). The results of differential analysis were analyzed by KEGG pathway enrichment analysis. The results showed that the processes of significant enrichment of high, medium and low atrazine concentrations compared with the control group was oxidative phosphorylation. The

transcription and translation related genes of elongation factor in ribosomes and SecY membrane protein related genes producing protein membrane channels were up-regulated, the F-Actin and V-ATPase related genes involved in transport in phagocytes were up-regulated, and the F-ATPase and V-ATPase related genes producing ATP during oxidative phosphorylation were up-regulated, indicating that the above related genes were involved in the corresponding response to atrazine stress. The stress response of *Suaeda* Heteroptera to atrazine stress is an energy consuming process. In this process, the expression of genes related to respiratory chain producing ATPase increases, the content of transcription and translation proteins of elongation factor in ribosome increases, and the expression of F-Actin and V-ATPase in phagosome increases. It is speculated that due to stress, a large number of body related proteins are transcribed and translated by elongation factors in ribosomes, and then proteins are transported through SecY membrane proteins, which are transported by phagocytes with the support of F-Actin and the catalysis of V-ATPase. At the same time, F-ATPase and V-ATPase supply a large amount of ATP during oxidative phosphorylation. NADH dehydrogenase affects the regulation of mitochondria on cell apoptosis guaranteeing the maintenance of system balance.

## Conclusion

The results of the difference analysis were subjected to KEGG PATHWAY enrichment analysis, and it was found that the processes that were significantly enriched at high, medium and low atrazine concentrations compared to the control were mainly: steroid biosynthesis, photosynthesis, protein processing in endoplasmic reticulum and oxidative phosphorylation. The genes related to F-actin and V-ATPase involved in transport in phagosome were up-regulated, and the genes related to F-ATPase and V-ATPase involved in ATP production in oxidative phosphorylation were up-regulated, indicating that all the above related process genes were involved in the corresponding response to atrazine stress. The stress response to atrazine stress is an energy-consuming process in which the expression of respiratory chain-related ATPase-generating genes increases, while the content of transcriptionally translated proteins of elongation factors in the ribosomes increases, and the expression of F-actin and V-ATPase both increase in the phagosomes. SecY membrane proteins produce channels in the membrane for protein transport, supported by F-actin and catalyzed by V-ATPase by phagosomes, while the oxidative phosphorylation process F-ATPase and V-ATPase supply large amounts of ATP, and NADH dehydrogenase affects the regulation of apoptosis by mitochondria to ensure the maintenance of system homeostasis.

A certain concentration of herbicides was found in the Panjin Red Beach wetland through monitoring, which originated from herbicides in the surrounding agricultural fields; it may have led to the degradation and even death of winged alkali ponies, so this study helps to further analyze the causes of its degradation.

**Declaration of competing interests.** The authors declare that they have no known competing financial interests or personal relationships that could have appeared to influence the work reported in this paper.

## REFERENCES

- [1] Alberto, D., Serra, A.-A., Sulmon, C., Gouesbet, G., Couée, I. (2016): Herbicide-related signaling in plants reveals novel insights for herbicide use strategies, environmental risk assessment and global change assessment challenges. – *Science of the Total Environment* 569-570:1618-1628.
- [2] Aviner, R. (2020): The Science of puromycin: from studies of ribosome function to applications in biotechnology. – *Computational and Structural Biotechnology Journal* 18: 1074-1083.
- [3] Bachetti, R. A., Urseler, N., Morgante, V., Damilano, G., Porporatto, C., Agostini, E., Morgante, C. (2021): Monitoring of atrazine pollution and its spatial-seasonal variation on surface water sources of an agricultural river basin. – *Bulletin of Environmental Contamination and Toxicology* 106: 929-935.
- [4] Banerjee, S., Kane, P. M. (2020): Regulation of V-ATPase activity and organelle pH by phosphatidylinositol phosphate lipids. – *Frontiers in Cell and Developmental Biology*, 8:510
- [5] Braun, H.-P. (2020): The oxidative phosphorylation system of the mitochondria in plants. – *Mitochondrion* 53(2020): 66-75.
- [6] Burstein, S. H., Rossetti, R. G., Yagen, B., Zurier, R. B. (2000): Oxidative metabolism of anandamide. – *Prostaglandins Other Lipid Mediat* 61(1-2): 29-41.
- [7] Cai, L., Liu, Z., Cai, L., Yan, X., Hu, Y., Hao, B., Xu, Z., Tian, Y., ..., Wan, J. (2022): Nuclear encoded elongation factor EF-Tu is required for chloroplast development in rice grown under low-temperature conditions. – *Journal of Genetics and Genomics* 5: 502-505.
- [8] Chakrapani, V., Patra, S. K., Mohapatra, S. D., Rasal, K. D., Deshpande, U., Nayak, S.,..., Barman, H. K. (2016): Comparative transcriptomic profiling of larvae and post-larvae of macrobrachium rosenbergii in response to metamorphosis and salinity exposure. – *Genes & Genomics* 38(11): 1061-1076.
- [9] Chen, B., Liu, X. G., Zheng, H. L., Liang, J. Y., Liang, N. C. (2009): Protein kinase CK2 $\alpha$ ' Screening of interacting protein NADH dehydrogenase 4. – *Chinese Tropical Medicine* 9(8): 1427-1428.
- [10] Chen, X. X., Ding, Y. L., Yang, Y. Q., Song, C. P., Wang, B. S., Yang, S. H., Guo, Y., Gong, Z. Z. (2021): Protein kinases in plant responses to drought, salt, and cold stress. – *Journal of Integrative Plant Biology* 63(1):53-78.
- [11] DeLey Cox, V. E., Cole, M. F., Gaucher, E. A. (2019): Incorporation of modified amino acids by engineered elongation factors with expanded substrate capabilities. – *ACS Synthetic Biology* 8(2): 287–296.
- [12] Eaton, A. F., Merkulova, M., Brown, D. (2021): The H(+)ATPase (v-ATPase): from proton pump to signaling complex in health and disease. – *American Journal of Physiology* 320(3):392-414.
- [13] Fan, H. (2009): Retroviruses. – *Encyclopedia of Microbiology* (Elsevier) 47: 519-534.
- [14] Fu, J. M., Momčilović, I., Vara Prasad, P. V. (2012): Roles of protein synthesis elongation factor EF-Tu in heat tolerance in plants. – *Journal of Botany* 2012(Article ID 835836):8.
- [15] Galkin, V. E., Orlova, Al., Schröder, G. F., Egelman, E. H. (2010): Structural polymorphism in F-actin. – *Nature Structural & Molecular Biology* 17(11):1318-1323.
- [16] Ge, J. Y., Liu, J., Wang, T. W., Huang, D., Li, J. W., Zhang, S., ..., Zhao, L. J. (2021): Prolonged exposure to the herbicide atrazine suppresses immune cell functions by inducing spleen cell apoptosis in rats. – *Ecotoxicology and Environmental Safety* 220:112386.
- [17] Harvey, W. R. (1992): Physiology of V-ATPases. – *Journal of Experimental Biology* 172(1): 1-17.

- [18] Hooper, K. M., Jacquin, E., Li, T., Goodwin, J. M., Brumell, J. H., Durgan, J., Florey, O. (2022): V-ATPase is a universal regulator of LC3-associated phagocytosis and non-canonical autophagy. – *The Journal of Cell Biology* 6.
- [19] Hughes, D. (2013): Elongation Factors: Translation. – *Brenner's Encyclopedia of Genetics* (Second Edition), 466-468.
- [20] James, A., Kumar, S. D. (2021): Atrazine detoxification by intracellular crude enzyme extracts derived from epiphytic root bacteria associated with emergent hydrophytes. – *Journal of Environmental Science and Health, Part B* 6.
- [21] Jaskolka, M. C., Kane, P. M. (2020): Interaction between the yeast RAVE complex and Vph1-containing Vo sectors is a central glucose-sensitive interaction required for V-ATPase reassembly. – *Journal of Biological Chemistry* 295(8):2259-2269.
- [22] Kakizawa, S., Oshima, K., Kuboyama, T., Namba, S. (2001): Cloning and expression analysis of phytoplasma protein translocation genes. – *Molecular Plant-Microbe Interactions (MPMI)* 14(9):1043-1050.
- [23] Kang, J., Ma, G. B., Yuan, L., Fu, Y. B., Li, F., Peng, C. S. (2021): Habitat suitability analysis of *Suaeda heteroptera* in coastal beach - Taking Caozhuang sea area of Xingcheng as an example. – *Marine Environmental Science* 2: 207-214.
- [24] Kang, W. J., Jiang, Z. H., Chen, Y. G., ..., Zhang, X. X. (2020): Plant transcriptome analysis reveals specific molecular interactions between alfalfa and its rhizobial symbionts below the species level. – *BMC Plant Biology* 20(1):293.
- [25] Karim, R., Reading, L., Dawes, L., Dahan, O., Orr, G. (2021): Transport of photosystem II (PS II)-inhibiting herbicides through the vadose zone under sugarcane in the Wet Tropics, Australia. – *Catena* 206:105527.
- [26] Kim, E. (2009): Postsynaptic development: Neuronal Molecular Scaffolds. – In: Binder, M. D. et al. (eds.) *Encyclopedia of Neuroscience*. Springer, Berlin, pp. 817-824.
- [27] Kühlbrandt, W. (2019): Structure and mechanisms of F-type ATP synthases. – *Annual Review of Biochemistry* 88(1):515-549.
- [28] Kumari, U., Banerjee, T., Singh, N. (2021): Evaluating ash and biochar mixed biomixtures for atrazine and fipronil degradation. – *Environmental Technology & Innovation* 23:101745.
- [29] Li, F. C., Cao, W. R., Wang, S. B., Cheng, H. Q., Zhao, C., Guan, M. (2008): Toxic effects of herbicide atrazine on *Scenedesmus obliquus* population. – *Anhui Agricultural Science* 17:7427-7428.
- [30] Li, J., Yu, X., Liu, Q., Ou, S., Xu, R. (2019): Screening of important lncRNAs associated with the prognosis of lung adenocarcinoma, based on integrated bioinformatics analysis. – *Molecular Medicine Reports* 19(5): 4067-4080.
- [31] Liu, S., Wei, H. F., Liu, C. F., Zhang, M. L., He, J., Gao, J., Zhao, Y. M. (2020): On site ecological restoration of *Suaeda heteroptera* in Panjin red beach. – *China wild plant resources* 6: 1-4.
- [32] Liu, Y., Song, C. W., Li, Y., Liu, Y., Song, J. M. (2011): The distribution of organochlorine pesticides (OCPS) in surface sediments of Bohai Sea Bay, China. – *Environmental Monitoring & Assessment* 184(4): 1921-1927.
- [33] Ludwig, N., Yerneni, S. S., Menshikova, E. V., Gillespie, D. G., Jackson, E. K., Whiteside, T. L. (2020): Author correction: simultaneous inhibition of glycolysis and oxidative phosphorylation triggers a multi-fold increase in secretion of exosomes: possible role of 2',3'-cAMP. – *Scientific Reports* 10:6948.
- [34] Ma, C., Wu, X., Sun, D., Park, E., Catipovic, M. A., ..., Li, L. (2019): Structure of the substrate-engaged SecA-SecY protein translocation machine. – *Nature Communications* 10(1):1-9.
- [35] Ma, L., Tymanskyj, S. R. (2020): Axon Growth and Branching. – *Cellular Migration and Formation of Axons and Dendrites* (Second Edition):57-58.

- [36] Mali, G. R., Verma, A., Malunjker, B. D. (2021): Effect of different post-emergence herbicides tank mix with atrazine on nutrient uptake and chlorophyll content in maize (*Zea mays* L.). – *Current Journal of Applied Science and Technology* 40(46):1-8.
- [37] Manoj, K. M. (2018): Aerobic respiration: criticism of the proton-centric explanation involving rotary adenosine triphosphate synthesis, chemiosmosis principle, proton pumps and electron transport chain. – *Biochemistry Insights* 11:1-23.
- [38] Manoj, K. M., Gideon, D. A., Parashar, A. (2020): What is the role of lipid membrane-embedded quinones in mitochondria and chloroplasts chemiosmotic Q-cycle versus murburn reaction perspective. – *Cell Biochemistry and Biophysics* 79(38):1-8.
- [39] McGuire, C. M., Forgac, M. (2018): Glucose starvation increases V-ATPase assembly and activity in mammalian cells through AMP kinase and phosphatidylinositide 3-kinase/Akt signaling. – *The Journal of Biological Chemistry* 293(23):9113-9123.
- [40] Mevy, J. P., Lloriod, B., Liu, X., Corre, E., Torres, M., Büttner, M.,..., Gauquelin, T. (2020): Response of downy oak (*Quercus pubescens* Willd.) to climate change: transcriptome assembly, differential gene analysis and targeted metabolomics. – *Plants* 9(9):1149.
- [41] Piccoli, C., Ripoli, M., Quarato, G., Scrima, R. (2008): Coexistence of mutations in pink1 and mitochondrial DNA in early onset parkinsonism. – *Journal of medical genetics* 45(9): 596.
- [42] Qi, W., Müller, B., Pernet-Coudrier, B., Singer, H., Liu, H., Qu, J., Berg, M. (2014): Organic micropollutants in the Yangtze River: seasonal occurrence and annual loads. – *Science of the Total Environment* 472: 789-799.
- [43] Rohr, J. R. (2021): The atrazine saga and its importance to the future of toxicology, science, and environmental and human health. – *Environmental Toxicology and Chemistry* 40(6):1544-1558.
- [44] Salazar, M. A., Kwiatkowski, A. V., Pellegrini, L. Cestra, G., Butler, M. H., Rossman, K. L.,..., De Camilli, P. (2003): Tuba, a novel protein containing bin/amphiphysin/Rvs and Dbl homology domains, links dynamin to regulation of the actin cytoskeleton. – *Journal of Biological Chemistry* 278(49):49031-43.
- [45] Stransky, L. A., Forgac, M. (2015): Amino acid availability modulates vacuolar H<sup>+</sup>-ATPase assembly. – *The Journal of Biological Chemistry* 290(45):27360-27369.
- [46] Guo J., Chen Y. Y, Lu P. Z.,et al.(2021).Roles of endophytic bacteria in *Suaeda salsa* grown in coastal wetlands: Plant growth characteristics and salt tolerance mechanisms. *Environmental Pollution* 287:117641.
- [47] Vasanthakumar, T., Rubinstein, J. L. (2020): Structure and roles of V-type ATPases. – *Trends in Biochemical Sciences* 45(4):295-307.
- [48] Wagh, D., Terry-Lorenzo, R., Waites, C. L., ..., Garner, C. C. (2015): Piccolo directs activity dependent F-actin assembly from presynaptic active zones via Daam1. – *PloS ONE* 10(4):e0120093.
- [49] Wang, Z. M., Niu, Y., Xu, J. Q., Sun, Z. J., Ding, Z. Q., Yang, X. Q. (2013): Cloning and sequence analysis of pollen protein elongation factor gene of heading cabbage. – *Journal of Horticulture* 10: 1990-1998.
- [50] Yan, Q. X., Zhao, P., Li, X., Zhang, M. H., Jiang, Y. J. (2015): Development trend and countermeasures of atrazine. – *Pesticides* 54(12): 933-936.
- [51] Zhang, H. Y., Hou, Z. H., Zhang, Y. L., Zhi, Y., Chen, J., Zhou, Y. B., Xu, Z. S. (2022): A soybean EF-Tu family protein GmEF8, an interactor of GmCBL1, enhances drought and heat tolerance in transgenic *Arabidopsis* and soybean. – *International journal of Biological Macromolecules (Elsevier)* 205:462-472.
- [52] Zhang, Y., Cao, B., Jiang, Z., Zhang, X. Y., Wang, Z. Y., Li, R. X. (2017): Effects of atrazine on enzyme activity and microbial diversity in black soil. – *Journal of Northeast Agricultural University* 48(3): 48-53.